Enhanced broadband piezoelectric energy harvesting using rotatable magnets

Shengxi Zhou,[1] Junyi Cao,[1,a)] Alper Erturk,[2] and Jing Lin[1]
[1]*State Key Laboratory for Manufacturing Systems Engineering, School of Mechanical Engineering, Xi'an Jiaotong University, Xi'an 710049, China*
[2]*G. W. Woodruff School of Mechanical Engineering, Georgia Institute of Technology, Atlanta, Georgia 30332, USA*

(Received 26 February 2013; accepted 15 April 2013; published online 29 April 2013)

We investigate a magnetically coupled nonlinear piezoelectric energy harvester by altering the angular orientation of its external magnets for enhanced broadband frequency response. Electromechanical equations describing the nonlinear dynamic behavior include an experimentally identified polynomial for the transverse magnetic force that depends on magnet angle. Up- and down-sweep harmonic excitation tests are performed at constant acceleration over the range of 0–25 Hz. Very good agreement is observed between the numerical and experimental open-circuit voltage output frequency response curves. The nonlinear energy harvester proposed in this work can cover the broad low-frequency range of 4–22 Hz by changing the magnet orientation. [http://dx.doi.org/10.1063/1.4803445]

Over the last decade, vibration-based energy harvesting has been investigated as a promising approach to enable self-sufficient wireless sensor nodes and portable small electronic devices due to the presence of vibrational energy in numerous natural and engineered systems.[1–5] Theoretical analyses and experimental validations of conventional linear-resonant energy harvesters have been reported by several research groups to generate the maximum power output under harmonic excitation.[6–9] However, these narrowband devices are not easy to implement in practice due to a number of issues that may cause mismatch between the excitation frequency and the resonance frequency, such as device imperfections due to manufacturing tolerances, changing ambient temperature (shifting the harvester's resonant frequency), or varying excitation frequency scenarios, resulting in drastic reduction of the power output. In order to overcome this issue, some researchers have focused on linear stiffness tuning schemes using an axial preload to match the excitation and resonance frequencies.[10,11] Applying magnetic force to alter the stiffness of the harvester by introducing nonlinearities is another option to enhance the frequency bandwidth.[12–20] Stanton *et al.*[12] obtained softening and hardening stiffness responses in a monostable piezoelectric energy harvester by changing the rectilinear position of external magnets. Erturk *et al.*[13,14] reported numerical and experimental investigations of a broadband bistable piezomagnetoelastic vibration energy harvester. An alternative bistable configuration based on magnetoelastic coupling was presented by Stanton *et al.*[15] along with detailed theoretical analyses of frequency-wise and amplitude-wise bifurcations. Lin *et al.*[16] proposed a magnetically coupled piezoelectric cantilever in which the displacement of the fixed magnet could be altered to achieve off-resonance vibration energy harvesting. Tang and Yang[17] studied a nonlinear piezoelectric energy harvester with a magnetic oscillator as a two-degree-of-freedom broadband energy harvester configuration. These efforts demonstrate frequency bandwidth and performance enhancement in vibration energy harvesters by leveraging magnetoelastic interactions in the context of our present work. Other efforts focusing on broadband energy harvesting can be found in review articles by Tang *et al.*,[18] Pellegrini *et al.*,[19] Westermann and Twiefel,[20] and Harne and Wang.[21]

Although the relative spacing and locations of the magnets have been well studied in bifurcations of magnetoelastic cantilevers,[12,15,22] the effect of angular orientation of the magnets remains uninvestigated. This letter presents an alternative nonlinear Broadband Piezoelectric Energy Harvester (BPEH) with rotatable magnets (Fig. 1) to further explore bandwidth enhancement by focusing on the magnet inclination angle. The BPEH device displayed in Fig. 1 consists of an elastic substrate, two symmetric piezoelectric layers at the root, tip magnet attachments, and external magnets. This system can exhibit bistable or monostable behavior over a range of frequencies depending on the angle α that the external magnets make with the horizontal. Additionally, this BPEH configuration can potentially save space since nonlinear frequency response can be altered by simply rotating the magnets rather than changing the magnet spacing (which would require more volume). Each one of the external magnets is embedded in a rotatable structure. The magnets at the tip of the cantilever can be used to change the resonant frequency while their interaction with the external magnets produces a magnetic force. The magnetoelastic interaction can be changed by adjusting the parameters d, h, and α. The objective of the present work is to explore the effect of α on the dynamic performance of the BPEH. For the fixed values of $d = 70$ mm and $h = 15.5$ mm in our experimental system, the magnet angles of $\alpha = 0^\circ$, 30°, 60°, and 90° are studied in the following.

For quantitative electromechanical modeling, a series discretization method (Rayleigh-Ritz method or assumed-modes method) is applied to the harvester based on the Euler–Bernoulli beam theory.[7,9,23] It should be noted from

a)Author to whom correspondence should be addressed. Electronic mail: caojy@mail.xjtu.edu.cn.

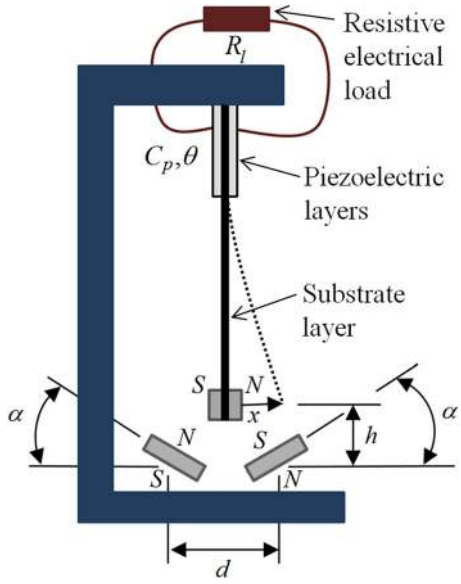

FIG. 1. Schematic of the BPEH with rotatable external magnets to study the effect of angle α on the broadband frequency response (d and h are fixed).

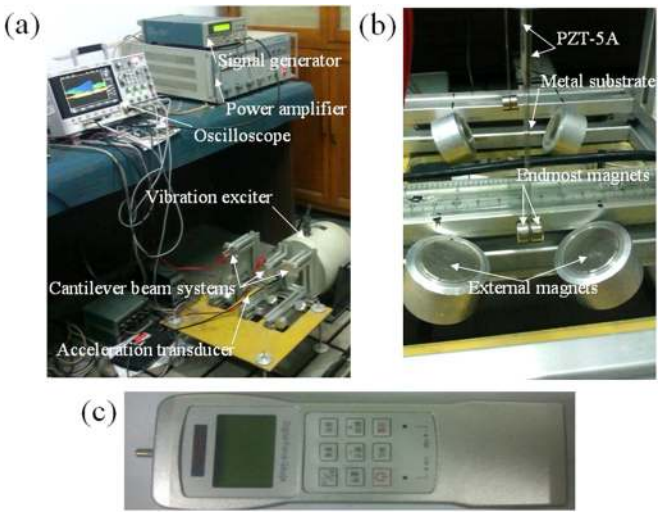

FIG. 2. (a) Overview of the experimental setup; (b) BPEH with close-up view of the magnets; and (c) small electronic dynamometer used for extracting the magnetic force under different magnet orientations.

Fig. 1 that the harvester becomes a linear resonant device if the external magnets are removed. For this linear configuration, the governing electromechanical equations (for the fundamental vibration mode) are

$$M\ddot{x} + C\dot{x} + Kx - \theta v = F, \tag{1}$$

$$C_p\dot{v} + \frac{v}{R_l} + \theta\dot{x} = 0, \tag{2}$$

where M is the equivalent mass, C is the equivalent damping, K is the equivalent stiffness, θ is the equivalent electromechanical coupling term, C_p is the equivalent capacitance of the piezoelectric layers, R_l is the load resistance, $v(t)$ is the voltage across the electrical load, $x(t)$ is the tip displacement of the harvester in the transverse direction, and $F(t)$ is the external mechanical force as the excitation term due to ambient vibrations.

The linear device described by Eqs. (1) and (2) becomes a magnetically coupled BPEH after adding the external magnets (Fig. 1). Representing the magnetic force as an external forcing term, the nonlinear equations of the BPEH become

$$M\ddot{x} + C\dot{x} + Kx - \theta v = F + F_m, \tag{3}$$

$$C_p\dot{v} + \frac{v}{R_l} + \theta\dot{x} = 0, \tag{4}$$

where F_m is the magnetic force in x direction that takes the empirical form of

$$F_m = \mu x + \lambda x^3, \tag{5}$$

which is experimentally identified by using a sensitive dynamometer. The coefficients of the magnetic force polynomial denoted by μ and λ depend on the angle α. It should be noted that the contribution of the magnetic force to the restoring force is $-F_m$ due to rearranging Eq. (3) in the alternative representation (yielding a total restoring force of $(K-\mu)x - \lambda x^3$ on the left hand side of Eq. (3)).

An overview of the experimental setup is shown in Fig. 2(a). The base excitation is produced by the experimental system consisting of a vibration exciter (JZK-40), a signal generator (AFG310), and a power amplifier (YE5874A). The accelerometer (AC135) is used to measure the base acceleration and quantify the excitation level while the experimental data are acquired by oscilloscope (MSOX3052A). The magnetic force F_m is measured by a micro dynamometer (HF-5) for different magnet angles. The metal substrate is made of stainless steel with the dimensions of $90 \times 15 \times 0.2$ mm^3. Each one of the two PZT-5A piezoceramic layers bracketing the substrate layer has the dimensions of $24 \times 15 \times 0.5$ mm^3. All of the four permanent magnets are NdFeB cylinder magnets, which can be seen in Fig. 2(b). The two tip magnets attached to the cantilever have a diameter of 10 mm and thickness of 5 mm, while the two external magnets have a diameter of 25 mm with the same thickness. Frequency sweep experiments are conducted close to open-circuit conditions of the BPEH (piezoelectric layers are connected to the 10 MΩ channel of the oscilloscope). The base acceleration values of $0.40g$ and $0.56g$ are selected as the two excitation levels. Linearly increasing frequency (up-sweep) and decreasing frequency (down-sweep) excitation experiments and simulations are performed slowly over the frequency range of 0–25 Hz.

In order to investigate the coupled system dynamics of the proposed BPEH, the magnetic force should be identified first. A dynamometer (Fig. 2(c)) is used to identify the transverse magnetic force (F_m) for different magnet angles (α) as a function of tip displacement. Polynomial fit of the form given by Eq. (5) is then applied to the identified magnetic force curves as depicted in Fig. 3. The markers in Fig. 3 show the experimental measurements while the curves are the polynomial fit representations for the magnet angles of $\alpha = 0°$, $30°$, $60°$, and $90°$. These polynomial fits are then used in the governing electromechanical equations to compare the numerical simulations with the experimental results. One should recall that the magnetic force term is on the right hand side of Eq. (3) as an *external force* in the present

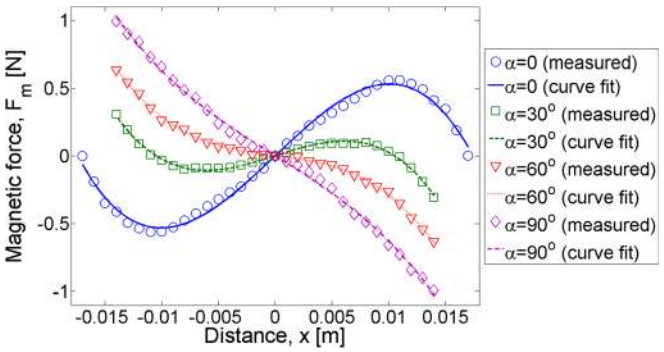

FIG. 3. Magnetic force curves versus transverse tip distance from the center line ($x = 0$) for different magnet angles (restoring force contribution from the magnetic force is $-F_m$).

representation. Therefore, the *restoring force* contribution would have the form of $-F_m$ on the left hand side of the same equation in the alternative form. It can be anticipated from the trends in Fig. 3 that both monostable-hardening and bistable characteristics can be realized depending on the magnet angle.

Experimental measurements and numerical simulations of the open-circuit voltage output frequency response are investigated next for different magnet angles. For $\alpha = 0^\circ$, the coefficients of the polynomial in Eq. (5) are $\mu = 79.17$ N/m, $\lambda = -260769.73$ N/m^3, and the BPEH device has two stable equilibrium positions in static condition, i.e., it is a bistable energy harvester. In this case, for the excitation level of $0.56g$ in up-sweep, the device has a frequency bandwidth of about 11.5 Hz dominated by large-amplitude periodic oscillations (Fig. 4) of the type originally suggested for energy harvesting by Erturk and Inman.[13,14] In this configuration, the maximum open-circuit voltage output can be as high as 43.2 V. Large-amplitude periodic response branch is observed in both numerical and experimental frequency response curves. When the excitation level is reduced to 0.40g, chaotic response is observed predominantly in the experimental and numerical results. We note that the up-sweep and down-sweep results are different and this difference can be pronounced dramatically for different initial conditions. In this configuration ($\alpha = 0^\circ$) involving chaotic and periodic response patterns over the frequency range of interest, the overall amplitude- and frequency-wise agreement between the numerical and experimental results is reasonable. Briefly, the experimental configuration has the wide bandwidth of 4–15.5 Hz for the magnet orientation of $\alpha = 0^\circ$.

For the magnet angle of $\alpha = 30^\circ$ (yielding $\mu = 26.71$ N/m and $\lambda = -241992.03$ N/m^3), the dynamic behavior of the BPEH is substantially altered as shown in Fig. 5. In this configuration of the external magnets, the predominant trend is strong hardening response. The bandwidth of the hardening behavior is increased as the excitation level is increased from $0.40g$ to $0.56g$ since the frequency of the up-sweep jump phenomenon[24] moves from 16.4 Hz to 17.2 Hz. The device generates a maximum voltage output of 30 V and offers an operating bandwidth of about 5 Hz in the experimental measurements. The overall trends in the numerical simulations and experimental measurements, including the hysteresis between up-sweep and down-sweep, are in good agreement. Therefore, by simple rotation of the magnets the operating bandwidth is further enhanced to 17.2 Hz in Fig. 5 as compared to the previous case (Fig. 4). Dominant superharmonic resonance of order three associated with cubic nonlinearity appears approximately around 4.5 Hz for $0.56g$ excitation (compare with the primary resonance, which is roughly near the down-sweep resonance). Superharmonic resonance frequencies can also be exploited in energy harvesting as suggested by Masana and Daqaq[25] although the present work is focused on the primary resonance behavior.

When the magnet angle is further modified, the broadband dynamics of the device is further altered as shown in Figs. 6 and 7 for the magnet angles of $\alpha = 60^\circ$ and $\alpha = 90^\circ$, respectively. The case of $\alpha = 60^\circ$ yields $\mu = -10.56$ N/m, $\lambda = -180938.52$ N/m^3 while $\alpha = 90^\circ$ results in $\mu = -52.47$ N/m, $\lambda = -104559.34$ N/m^3 for the polynomial expression of the magnetic force in Eq. (5). The up-sweep jump frequency associated with nonlinear hardening behavior is moved to 22 Hz in the extreme case of $\alpha = 90^\circ$. It should be noted that the hysteresis between up-sweep and down-sweep in the nonlinear frequency response diminishes as α increases. Indeed, the narrowest bandwidth among the four cases considered in this work is obtained for $\alpha = 90^\circ$. Overall, as the magnet angle is altered from $\alpha = 0^\circ$ to $\alpha = 90^\circ$, the BPEH investigated herein covers the frequency

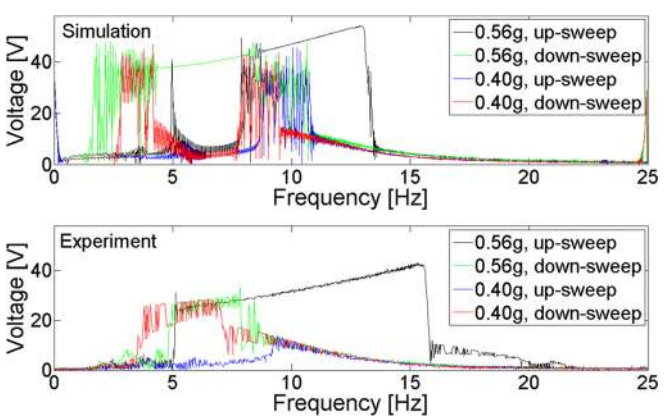

FIG. 4. Numerical and experimental up-sweep and down-sweep open-circuit voltage output frequency response curves for $\alpha = 0^\circ$ ($\mu = 79.17$ N/m, $\lambda = -260769.73$ N/m^3) at two excitation levels.

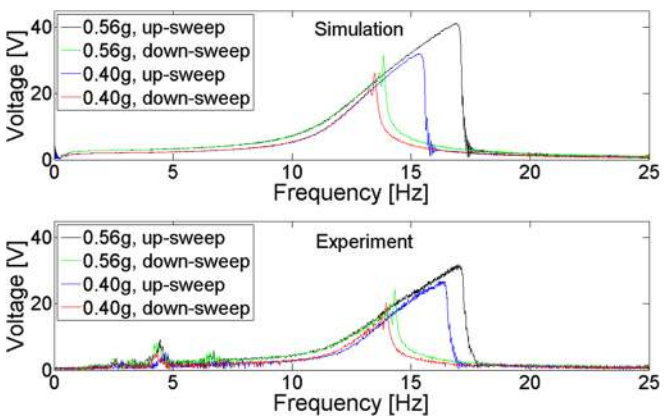

FIG. 5. Numerical and experimental up-sweep and down-sweep open-circuit voltage output frequency response curves for $\alpha = 30^\circ$ ($\mu = 26.71$ N/m, $\lambda = -241992.03$ N/m^3) at two excitation levels.

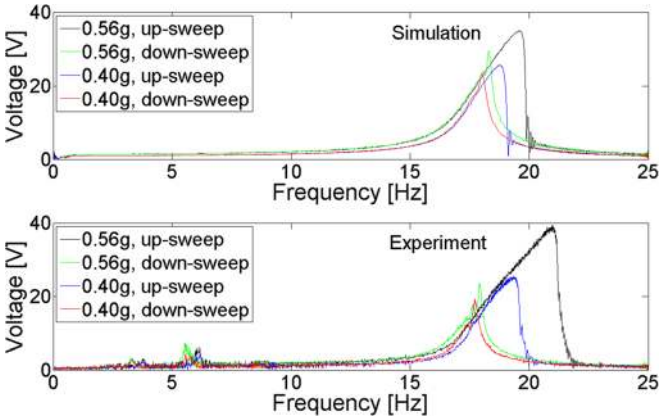

FIG. 6. Numerical and experimental up-sweep and down-sweep open-circuit voltage output frequency response curves for $\alpha = 60^\circ$ ($\mu = -10.56$ N/m, $\lambda = -180938.52$ N/m^3) at two excitation levels.

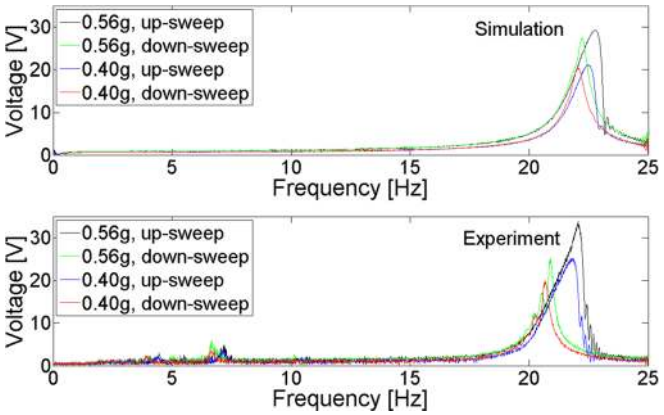

FIG. 7. Numerical and experimental up-sweep and down-sweep open-circuit voltage output frequency response curves for $\alpha = 90^\circ$ ($\mu = -52.47$ N/m, $\lambda = -104559.34$ N/m^3) at two excitation levels.

range of 4–22 Hz with large amplitude response, offering a wide bandwidth of 18 Hz without substantially changing the device architecture. The evolution of 1:3 superharmonic resonance as the magnet angle is changed from $\alpha = 30^\circ$ to $\alpha = 90^\circ$ (Figs. 5–7) is noteworthy.

In summary, the nonlinear BPEH experimentally and numerically explored in this work can exhibit enhanced broadband performance in piezoelectric power generation based on rotatable external magnets. The results indicate that the magnet inclination angle plays a vital role in broadening the operating bandwidth and changing the dynamic characteristics of the magnetically coupled BPEH (from bistable to monostable Duffing oscillator behavior). In addition to an overall wide bandwidth of 4–22 Hz obtained for different magnet angles in open-circuit condition, the advantage of the configuration investigated in the present work is that it does not require much auxiliary space since the BPEH dynamics is achieved by rotating the magnets only rather than translating them relative to each other.

This project has been supported by the Natural Science Foundation of China (Grant No. 51075317) and Program for New Century Excellent Talents in University (Grant No. NCET-12-0453).

[1]N. S. Hudak and G. G. Amatucci, J. Appl. Phys. **103**, 101301 (2008).
[2]K. A. Cook-Chennault, N. Thambi, and A. M. Sastry, Smart Mater. Struct. **17**, 043001 (2008).
[3]D. P. Arnold, IEEE Trans. Magn. **43**, 3940 (2007).
[4]S. R. Anton and H. A. Sodano, Smart Mater. Struct. **16**, R1–R21 (2007).
[5]H. Liu, S. Zhang, R. Kathiresan, T. Kobayashi, and C. Lee, Appl. Phys. Lett. **100**, 223905 (2012).
[6]S. Roundy and P. K. Wright, Smart Mater. Struct. **13**, 1131 (2004).
[7]N. E. duToit and B. L. Wardle, AIAA J. **45**, 1126–1137 (2007).
[8]A. Erturk and D. J. Inman, Smart Mater. Struct. **18**, 025009 (2009).
[9]A. Erturk and D. J. Inman, *Piezoelectric Energy Harvesting* (Wiley, Chichester, UK, 2011).
[10]E. S. Leland and P. K. Wright, Smart Mater. Struct. **15**, 1413 (2006).
[11]Y. Hu, H. Xue, and H. Hu, Smart Mater. Struct. **16**, 1961 (2007).
[12]S. C. Stanton, C. C. McGehee, and B. P. Mann, Appl. Phys. Lett. **95**, 174103 (2009).
[13]A. Erturk, J. Hoffmann, and D. J. Inman, Appl. Phys. Lett. **94**, 254102 (2009).
[14]A. Erturk and D. J. Inman, J. Sound Vib. **330**, 2339 (2011).
[15]S. C. Stanton, C. C. McGehee, and B. P. Mann, Physica D **239**, 640–653 (2010).
[16]J. T. Lin, B. Lee, and B. Alphenaar, Smart Mater. Struct. **19**, 045012 (2010).
[17]L. H. Tang and Y. W. Yang, Appl. Phys. Lett. **101**, 094102 (2012).
[18]L. Tang, Y. Yang, and C. K. Soh, J. Intell. Mater. Syst. Struct. **21**, 1867–1897 (2010).
[19]S. P. Pellegrini, N. Tolou, M. Schenk, and J. L. Herder, "Bistable vibration energy harvesters: A review," J. Intell. Mater. Syst. Struct. (in press).
[20]J. Twiefel and H. Westermann, "Survey on broadband techniques for vibration energy harvesting," J. Intell. Mater. Syst. Struct. (in press).
[21]R. L. Harne and K. W. Wang, Smart Mater. Struct. **22**, 023001 (2013).
[22]F. C. Moon and P. J. Holmes, J. Sound Vib. **65**, 275–296 (1979).
[23]A. Erturk, Comput. Struct. **106–107**, 214–227 (2012).
[24]A. H. Nayfeh and D. T. Mook, *Nonlinear Oscillations* (Wiley, New York, 1979).
[25]R. Masana and M. F. Daqaq, J. Appl. Phys. **111**, 044501 (2012).